Monzón Baeza, V. & García Armada, A. (2019). Non-Coherent Massive SIMO System Based on M-DPSK for Rician Channels. *IEEE Transactions on Vehicular Technology*, 68(3), 2413-2426.

DOI: 10.1109/tvt.2019.2892390

Non-Coherent Massive SIMO System based on M-DPSK for Rician Channels

Victor Monzon Baeza, *Student Member, IEEE* and Ana Garcia Armada, *Senior Member, IEEE*

***Abstract*—In this paper we propose a new constellation design for a non-coherent massive single input multiple output (m-SIMO) uplink system based on M-DPSK suitable for Rician channels. Under Rician propagation, the non-coherent systems proposed until now cannot completely remove the interference. This new design takes into account the inter user and inter symbol interferences in order to convert them into useful terms which help us in the non-coherent detection. We propose an algorithm to non coherently detect the joint symbol with the information from all users leveraging the characteristics of the new constellation. In addition, the signal to interference plus noise ratio is derived and is used to present analytical bounds for the symbol error rate. It is shown that the analytical results tightly match the numerical simulation. We show that with the proposed constellation and detection algorithm we are able to leverage the LOS component of the Rician propagation, obtaining a better performance than with Rayleigh channels.**

***Index Terms*—Massive MIMO, Differential PSK, 5G system, non-coherent detection, Rician channel.**

I. Introduction

The explosive usage of rich multimedia content in wireless devices has overloaded the communication networks. This has resulted in a remarkable spectrum crisis in the overcrowded radio frequency bands. Hence, there is a need for searching alternate techniques with more spectral efficiency to accommodate the needs of emerging wireless communications systems.

Massive Multiple Input Multiple Output (m-MIMO) systems are becoming one of the key enabling technologies for future 5G communication systems and beyond [1], [2]. They provide high spectral- and energy-efficiency thanks to the deployment of a large number of antennas in the base station (BS), far beyond those used in the current operational standards [3]. In addition, novel nonorthogonal multiple access techniques are proposed for 5G radio networks such as pattern division multiple access (PDMA) which also improves the spectrum efficiency over classical orthogonal techniques [4].

Two drawbacks of m-MIMO are the high overhead to obtain channel state information (CSI) and the pilot contamination [5]. To solve these issues, an interesting consideration for next generation communications is the use of differential encoding and non-coherent (NC) detection [6]. Several previous works have proposed designs for non-coherent massive Single Input Multiple Output (NC m-SIMO) [7]-[11]. In [7] designs based on energy detection are presented, with the drawback that the number of antennas is excessive even for m-MIMO. In [8], coding schemes are included to reduce this number but the reduction is not enough when attaining a reasonable performance. The authors in [9] focused on uniquely factorable constellations for NC detection that are not developed for m-MIMO yet. These designs work well in the high signal to noise ratio (SNR) regime and for single-user systems. As an alternative to the energy-detection approaches, several schemes based on Differential Quaternary Phase Shift Keying (DQPSK) have been proposed [10]. In [11], we proposed introducing a coding scheme based on bit-interleaved coded modulation and iterative decoding (BICM-ID) which allowed decreasing the number of antennas a 90% with respect to the case without coding. Our proposal outperformed the benchmarks of [7], [8] and [10].

These works focused on Rayleigh fading. However, current scenarios such as rural or suburban environments, backhaul wireless systems [12], and even new device-to-device (D2D) communications [13] can have a predominant line-of-sight (LOS) component, so that they are better modeled by Rician fading [14], [15]. The same happens when using higher frequencies, looking for wider spectrum availability, such as in millimeter frequency bands. In [7], some performance results for a single-user system were shown for Rician channels. The constellation was built depending on the statistics of the channel, while in our DPSK aided design [11] the constellation is fixed and independent of the statistics of the channel as we showed in [16] for the same channel conditions as in [7]. That is, using a design based on DPSK constellation the statistics of the channel do not need to be known. Furthermore, in [16] a gain with respect to other works that also consider Rician channel was shown both for different numbers of required antennas and spectral efficiency.

For multi-user scenarios with Rician fading, the designs in [10] and [11], originally proposed for Rayleigh fading, are no longer valid when we consider Rician fading due to the fact that the LOS component generates inter user interference (IUI) and inter symbol interference (ISI) when these designs are used under such propagation conditions. Therefore, the constellation scheme has to be redesigned in order to counteract as much as possible these effects of the LOS channel component. [17], [18] analyze the behavior of coherent massive MIMO in Rician channels and stress the importance of considering these specific propagation characteristics that may happen in realistic scenarios. Now, in this contribution we consider them for the non-coherent systems.

In the area of the NC detection, often the correlation between the phase distortions experienced by the consecutively transmitted symbols is exploited by jointly processing the received multiple symbols in order to improve the system performance [6]. The authors in [19] presented a multiple

This work has been partially funded by the Spanish National Project TERESA-ADA (TEC2017-90093-C3-2-R) (MINECO/AEI/FEDER, UE). The authors are with University Carlos III of Madrid, Spain, e-mail: vmonzon@tsc.uc3m.es and agarcia@tsc.uc3m.es

symbol differential detector for m-SIMO which is not valid either for Rician fading channels nor multi-user systems as we will show. Here, we will demonstrate that a multiple-symbol detection is not enough to compensate the interference unless we carefully select a new constellation design. In addition, the large number of antennas is not sufficient neither to cancel the IUI and ISI with the resources proposed in [11]. Therefore, we have to find an algorithm to cancel these terms.

The novel contribution of this work is that based on the analysis of the behavior of the NC m-SIMO systems when we have a Rician fading, we present a new constellation design to overcome the problem of the LOS channel component. Furthermore we develop a decoding algorithm that taking into account the characteristics of the new constellation and interference, outperforms exiting algorithms for NC detection. In addition, we propose some guidelines to design other constellations for NC m-SIMO systems based on DPSK modulation. We further illustrate the system performance, demonstrating that the proposed algorithm outperforms the previous work based on energy detection, so it can be a good choice for the evolution of wireless communications systems.

The rest of the paper is organized as follows. In Section II the system model is presented. The interference is analyzed in Section III. The new constellation design is shown and analyzed in Section IV. The new detection algorithm is proposed in Section V. In Section VI the performance is analyzed and compared to previous work. Finally, Section VII presents the conclusions.

Notation: The following notation will be used in this paper. Boldface symbols will be used for matrices and vectors, while italic letters will be used for scalars. Superscripts $^{\mathrm{T}}$ and $^{\mathrm{H}}$ denote the transpose and the Hermitian transpose of a matrix, respectively, while * is the conjugate of a scalar. $E\{\cdot\}$ denotes expectation. The μ-mean circularly symmetric complex Gaussian distribution with variance σ^2 is denoted as $CN(\mu,\sigma^2)$. $\Re\{\cdot\}$ denotes the real part of a complex number.

II. System Model

We consider a multi-user SIMO uplink scenario, where a single base station (BS) is equipped with R receive antennas (RA) to receive the signals transmitted from J mobile stations (MSs), or users. In particular, we focus on $J=2$ users as shown in Fig. 1. The design proposed for this scheme is valid for more users, however as it will be shown in the performance analysis in Section VI, the more users the higher numbers of RA at the BS are required. Hence, for achieving a system with more users we can employ orthogonal techniques such as Time Division Multiplex Access (TDMA). This system model could apply to a beyond 5G cellular network where several users are communicating with the BS. It could also represent a wireless backhaul where several BS are transmitting towards a central baseband unit (BBU), or even an evolved Wireless Fidelity (WiFi) system where several terminals are accessing the access point. In all these scenarios it is likely that the channel follows Rician fading. This kind of non coherent schemes have been shown to work well both under static channels and realistic time-varying conditions [20].

A user j transmits a signal $x_j[n]$ at time instant n, which is a differentially encoded version of $s_j[n]$ formulated as

$$x_j[n] = s_j[n]x_j[n-1],\ n>1. \tag{1}$$

A set of p bits, $b_1,...,b_p$, are grouped in the symbols $s_j[n]$ that belong to an M-ary PSK constellation, $\mathfrak{M}_j=\{s_{m,j},\ m=0,1,...,\ M-1\}$, where $|s_{m,j}[n]|=1$ and M is the order of the constellation defined as $M=2^p$. The $x_j[0]$ is a first symbol known at the transmitter and receiver which is taken from the constellation $\mathfrak{M}_j$. The m-MIMO wireless channel is modeled by the $(R\times J)$-element channel matrix $\widetilde{\boldsymbol{H}}=\boldsymbol{H}+\mu$, whose components $\widetilde{h_{rj}}$ represent the propagation from the user j-th to the r-th antenna of the BS. These elements $\widetilde{h}_{rj}=h_{rj}+\mu$, where $h_{rj}\sim CN(0,\sigma_h^2)$, are circularly symmetric complex Gaussian random variables. Hence, we have extracted the mean of the channel μ to remark the effect of the LOS channel component in the expressions. We assume that the statistics of the channel are defined as follows

$$\mu^2=\frac{K}{K+1} \tag{2}$$

and

$$\sigma_h^2=\frac{1}{K+1}, \tag{3}$$

where K is the Rician factor ($K>0$), which characterizes the fading model [21]. This factor characterizes a propagation with LOS between the BS and the user. Note that when K=0 we have a Rayleigh channel in which there is no dominant propagation along the LOS and in this case, the system model is equivalent to that presented in [11]. For simplicity of the presentation, we assume that all the channels experience Rician fading with the same K-factor. The $(R\times 1)$-element vector $\boldsymbol{y}[n]$ groups the signals received in each of the BS antennas at time instant n. Then, $\boldsymbol{y}[n]$ is obtained as follows

$$\boldsymbol{y}=\widetilde{\boldsymbol{H}}\boldsymbol{x}+\boldsymbol{\nu}, \tag{4}$$

where we will remove the time dependency n to facilitate the notation. Here the AWGN is represented by the $(R\times 1)$-element vector $\boldsymbol{\nu}$, $\nu_r[n]\sim CN(0,\sigma^2)$.

The power of the signal received at each antenna is

$$E\{||\widetilde{\boldsymbol{H}}\boldsymbol{x}||^2\}=\sum_{j=1}^{J}|s_j|^2(\sigma_h^2+\mu^2)=J, \tag{5}$$

as $|s_j|^2=1$ and $(\sigma_h^2+\mu^2)=1$, then we define the reference SNR as

$$\rho=\frac{E\{||\widetilde{\boldsymbol{H}}x||^2\}}{\sigma^2}=\frac{(\sigma_h^2+\mu^2)J}{\sigma^2}=\frac{J}{\sigma^2}. \tag{6}$$

At the receiver shown in Fig. 1, we assume that $h_{rj}[n-1]=h_{rj}[n]=h_{rj},\ r=1,...,R$ and $j=1,...,J$, meaning that the channel stays time-invariant for two consecutive symbols. [1] Hence, the phase difference is non-coherently detected for these two symbols received at each antenna. The resulting received symbol is the decision variable $z[n]$ defined as follows

[1] In a real scenario there will be a small variation between these two channels, this is just an assumption for the analysis. It is shown in [19] that our scheme is very robust to the channel variability that is likely to happen in realistic scenarios.

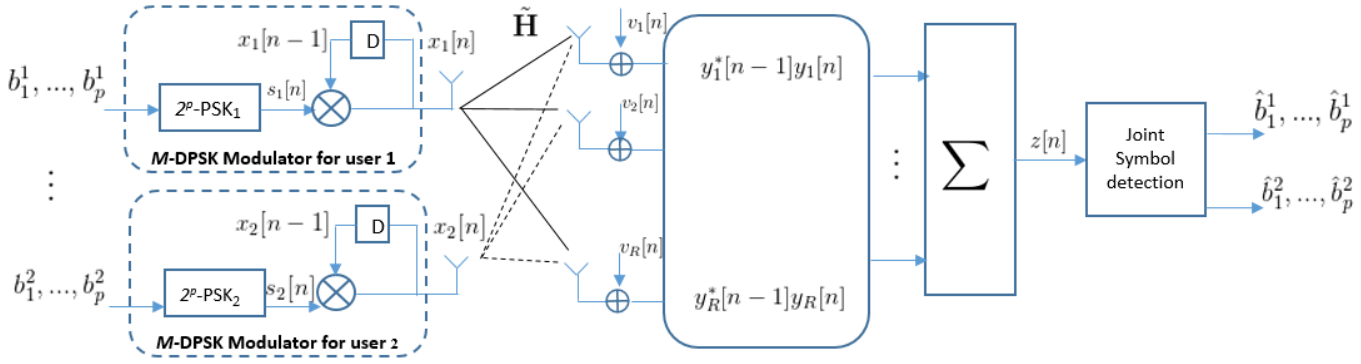

Fig. 1. Non-Coherent m-SIMO system model for $J = 2$ users.

$$z[n] = \frac{1}{R}\sum_{r=1}^{R} y_r[n-1]^* y_r[n], \tag{7}$$

that contains information and interference gleaned from all antennas. This variable is more detailed in (8) in the next page. We observe that the terms obtained for the Rayleigh case in [11] must be recalculated for the new channel statistics defined in (2) and (3). Also, we find new terms which will create additional interference and will be taken into account to design new constellations. Using the Law of Large Numbers [23] from (8) we can see that the old terms are now

$$\frac{1}{R}\sum_{r=1}^{R} |h_{rj}|^2 \overset{R\to\infty}{=} \sigma_h^2, \tag{9}$$

$$\frac{1}{R}\sum_{r=1}^{R} \Re\{h_{rj}\} \overset{R\to\infty}{=} 0, \tag{10}$$

and the new terms obey

$$\frac{1}{R}\sum_{r=1}^{R}\sum_{j=1}^{J}\sum_{\substack{k=1\\k\neq j}}^{J} \mu h_{rj} x_j[n] x_k^*[n-1] \overset{R\to\infty}{=} 0, \tag{11}$$

$$\frac{\mu}{R}\left[\sum_{r=1}^{R} x_j^*[n-1]v_r[n] + \sum_{r=1}^{R} x_j[n]v_r^*[n-1]\right] \overset{R\to\infty}{=} 0, \tag{12}$$

almost surely. In addition, taking into account $(\sigma_h^2 + \mu^2) = 1$, then we have

$$z[n] \overset{R\to\infty}{=} \sum_{j=1}^{J} s_j[n] + \ interfering\ terms \tag{13}$$

We define the joint symbol as

$$\varsigma[n] = \sum_{j=1}^{J} s_j[n] \tag{14}$$

which shapes the joint constellation in the receiver side. This constellation $\mathfrak{M} = \{\varsigma_k, k = 0, ..., \mathfrak{K}\}$ of cardinality $\mathfrak{K} = M^J$ is obtained from adding combinations of the constellation points of all $\mathfrak{M}_j$ as $\{s_{m^{(1)},1} + s_{m^{(2)},2} + ... + s_{m^{(j)},J}, m^{(j)} = 0, 1, ..., M-1\}$. In Section IV we will show more details on criteria to design the constellations. Then as R grows bigger, we have (13) can be approximated as

$$z[n] \overset{R\to\infty}{=} \varsigma[n] + \ interfering\ terms \tag{15}$$

Due to the fact that the channel contains a LOS component the number of interfering terms which cause IUI increases with respect to the Rayleigh case. Particularly, the interfering terms include a new one not dependent on R called useful interfering term (UIT) defined as

$$UIT[n] = \sum_{j=1}^{J}\sum_{\substack{k=1\\k\neq j}}^{J} x_j[n] x_k^*[n-1]. \tag{16}$$

Consequently we analyse this term because we will be able to convert part of the IUI into a useful term for the non-coherent detection. In Section IV, we will show how to consider the characteristics of the UIT in the constellation design in order to improve the performance in the Rice channels with respect to Rayleigh channels. Based on this new design which accounts for the UIT, the Joint Symbol Detection (JDS) block can obtain an estimate of $\varsigma[n]$ from $z[n]$ as explained in Section V and efficiently recover the users data $s_j[n]$ from the jointly detected symbol $\hat{\varsigma}[n]$.

III. Analysis of The Signal To Interference Plus Noise Ratio

The Signal to Interference plus Noise Ratio (SINR) is defined as the ratio of the signal power to the power of AWGN noise plus interference. When detecting $\hat{\varsigma}[n]$ from $z[n]$, the interference plus noise arises from the interfering terms in (15) and from equalities in (9)-(12) not being met due to a finite value of R. Hence the interference plus noise term $i[n]$ is shown in (17) in the next page.

We analyze the power of the different terms of $i[n]$, $I = E\{|i[n]^2|\}$ in the Appendix A with more details. We further demonstrate in the Appendix A that all interfering terms $i[n]$ are independent from one another so the total interference power I is the sum of the individual powers. Due to the fact that there is one term of interference (UIT) which does not depend on R, contrary to the others that in general decrease with R, we study the SINR for the following different cases.

$$z[n] = \frac{1}{R}\sum_{j=1}^{J}\sum_{r=1}^{R}[|h_{rj}|^2 + 2\mu\Re\{h_{rj}\} + \mu^2]s_j[n] + \underbrace{\mu^2\sum_{j=1}^{J}\sum_{\substack{k=1\\k\neq j}}^{J} x_j[n]x_k^*[n-1]}_{\text{term not dependent on } R,\ (UIT)\ \text{due to the LOS component}}$$
$$+ \underbrace{\frac{1}{R}\sum_{r=1}^{R}\sum_{j=1}^{J}\sum_{\substack{k=1\\k\neq j}}^{J} h_{rj}h_{rk}^*x_j[n]x_k^*[n-1] + \frac{1}{R}\sum_{j=1}^{J}\sum_{r=1}^{R} h_{rj}x_j[n]v_r^*[n-1] + \frac{1}{R}\sum_{j=1}^{J}\sum_{r=1}^{R} h_{rj}^*x_j^*[n-1]v_r[n] + \frac{1}{R}\sum_{r=1}^{R} v_r[n]v_r^*[n-1]}_{\text{old terms also present in the Rayleigh case}} \quad (8)$$
$$+ \underbrace{\frac{1}{R}\sum_{r=1}^{R}\sum_{j=1}^{J}\sum_{\substack{k=1\\k\neq j}}^{J} \mu h_{rj}x_j[n]x_k^*[n-1] + \frac{1}{R}\sum_{r=1}^{R}\sum_{j=1}^{J}\sum_{\substack{k=1\\k\neq j}}^{J} \mu h_{rj}^*x_j^*[n-1]x_k[n] + \frac{\mu}{R}[\sum_{r=1}^{R}\sum_{j=1}^{J} x_j[n]v_r^*[n-1] + \sum_{r=1}^{R}\sum_{j=1}^{J} x_j^*[n-1]v_r[n]]}_{\text{new terms due to the LOS component}}$$

A. SINR with unknown UIT

In order not to increase the complexity in the receiver with respect to the Rayleigh case, we consider the UIT is totally unknown in the detection procedure. Since it can not be removed by increasing the number of antennas R, the total interference will be increased due to the lack of knowledge of this term. We consider this case as a worst performance bound. Consequently, we will have to include the power of UIT (I_{UIT}) in the total interference. By exploiting the properties of Gaussian and Wishart matrices, the expectation of the power of the different terms of $i[n]$ can be obtained. The first four terms have been already obtained in [11]. However, the value of some of them is different because here $\sigma_h^2 \neq 1$. They are as follows

$$I_0 = \frac{J^2\sigma_h^2\mu}{R} \quad (18)$$

$$I_1 = \frac{\sigma_h^4 J}{R} \quad (19)$$

$$I_2 = \frac{2\sigma_h^2\sigma^2 J}{R} \quad (20)$$

$$I_3 = \frac{\sigma^4}{R}. \quad (21)$$

The power of the new terms which appear due to the non-zero mean of the channel are

$$I_4 = \frac{2\mu^2 J(J-1)\sigma_h^2}{R} \quad (22)$$

$$I_5 = \frac{2\mu^2\sigma^2 J}{R}. \quad (23)$$

Similarly, the interfering power due to the UIT is

$$I_{UIT} = J(J-1)\mu^4, \quad (24)$$

then the total interference is formulated as

$$I_{total}^{worst} = \sum_{i=0}^{5} I_i + I_{UIT}, \quad (25)$$

the SINR that we can achieve is

$$SINR_{worst} = \frac{E\{||\widetilde{\boldsymbol{H}}x||^2\}}{I_{total}^{worst}} = \frac{(\mu^2+\sigma_h^2)JR}{J(J-1)\mu^4R + J\sigma_h^2(J\mu+\sigma_h^2+2\mu^2(J-1)) + 2\sigma^2J(\mu^2+\sigma^2)+\sigma^4} \quad (26)$$

since $(\mu^2+\sigma_h^2)$ is equal to 1 then the SINR for the worst case can be reduced to

$$SINR_{worst} = \frac{JR}{J(J-1)\mu^4R + J\sigma_h^2(J\mu+\sigma_h^2+2\mu^2(J-1)) + 2\sigma^2J+\sigma^4} \quad (27)$$

We can now propose two approximations for the low and high SNR regimes, that is when either the self- interference or the AWGN noise contributions are dominant. For high SNR we have that only I_{UIT} is significant and constant (independently of R), so that

$$SINR_{worst}^{H} = \frac{1}{(J-1)\mu}, \quad (28)$$

while for low SNR (29), the main dominant term is I_5 which does not depend on the Rice factor K, matching with the Rayleigh case. Since we are interested in the low SNR regime, we can see that our system is independent of the channel statistics for low ρ.

$$SINR_{worst}^{L} = \frac{RJ}{\sigma^4}. \quad (29)$$

As we can see in Fig. 2, the SINR when we can not estimate the UIT matches the theoretical expression in (27) for $R = 100$ and 1000 antennas. Note that as ρ increases the SINR is limited by the UIT value which depends on the Rician factor K but not on the number of antennas. Also the bounds for high and low K are shown.

B. SINR with perfectly known UIT

In this case, we consider that the UIT is correctly estimated using the best detection algorithm at the cost of an increased receiver complexity. This is just considered in this subsection for obtaining a performance bound that we will try to achieve

$$i[n] = z[n] - \varsigma[n] = \underbrace{\frac{1}{R}\sum_{j=1}^{J}(\sum_{r=1}^{R}[|h_{rj}|^2 + 2\mu\Re\{h_{rj}\} + \mu^2] - 1)s_j[n]}_{i_0[n]} + \underbrace{+\frac{1}{R}\sum_{r=1}^{R}\sum_{j=1}^{J}\sum_{\substack{k=1\\k\neq j}}^{J} h_{rj}h_{rk}^{*}x_j[n]x_k^{*}[n-1]}_{i_1[n]}$$

$$+\underbrace{\frac{1}{R}\sum_{j=1}^{J}\sum_{r=1}^{R} h_{rj}x_j[n]v_r^{*}[n-1]}_{i_2[n]} + \underbrace{\frac{1}{R}\sum_{j=1}^{J}\sum_{r=1}^{R} h_{rj}^{*}x_j^{*}[n-1]v_r[n]}_{i_2[n]} + \underbrace{\frac{1}{R}\sum_{r=1}^{R} v_r[n]v_r^{*}[n-1]}_{i_3[n]} + \underbrace{\sum_{j=1}^{J}\sum_{\substack{k=1\\k\neq j}}^{J}\mu^2 x_j[n]x_k^{*}[n-1]}_{(useful)\ interference\ term} \tag{17}$$

$$+\underbrace{\frac{\mu}{R}\sum_{r=1}^{R}\sum_{j=1}^{J}\sum_{\substack{k=1\\k\neq j}}^{J} h_{rj}x_j[n]x_k^{*}[n-1] + \frac{\mu}{R}\sum_{r=1}^{R}\sum_{j=1}^{J}\sum_{\substack{k=1\\k\neq j}}^{J} h_{rj}^{*}x_j^{*}[n-1]x_k[n]}_{i_4[n]} + \underbrace{\frac{\mu}{R}[\sum_{r=1}^{R}\sum_{j=1}^{J} x_j[n]v_r^{*}[n-1] + \sum_{r=1}^{R}\sum_{j=1}^{J} x_j^{*}[n-1]v_r[n]]}_{i_5[n]}$$

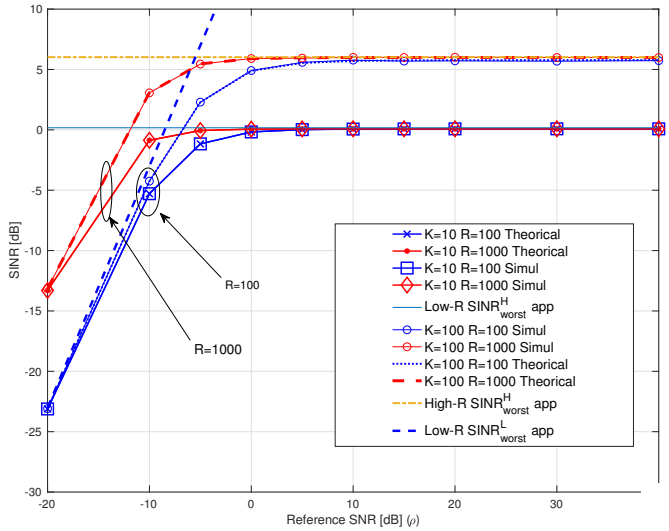

Fig. 2. SINR for unknown UIT case (worst case).

with our designs in Section IV. Consequently, we can ign that term to derive the total interference as $I_{total}^{ideal} = \Sigma_{i=}^{5}$ Then the SINR obeys

$$SINR_{ideal} = \frac{E\{||\widetilde{\boldsymbol{H}}x||^2\}}{I_{total}^{ideal}} \quad (\\ = \frac{JR}{J\sigma_h^2(J\mu+\sigma_h^2+2\mu^2(J-1))+2\sigma^2 J+\sigma^4}$$

We propose two approximations for the low and high Sl regimes as well. For high SNR we have that only I_0 significant, so that

$$SINR_{ideal}^{H} = \frac{R}{J\mu\sigma_h^2}, \quad ($$

while for low SNR (32), the main dominant term is I_3 which does not depend on the Rice factor K, matching with the Rayleigh case and worst case. Again, we can see as our system is independent of the channel statistics for low ρ.

$$SINR_{ideal}^{L} = \frac{RJ}{\sigma^4}. \tag{32}$$

From equations (30)-(32) we can see that increasing the number of antennas at the BS the SINR increases in the same proportion. That is, the energy efficiency scales as R, the same scaling law as for coherent systems with perfect CSI, while for coherent systems with non-perfect CSI the energy efficiency scales as $\sqrt{R}$ [22].

Fig. 3 shows the SINR obtained by simulation and the theoretical values for $J = 2$ users, K =10, 100 and 1000, where we can see the perfect agreement with (30) and the approximations (31) and (32). Once, again we can see that Rice and Rayleigh cases are identical for low SNR. Conversely, we have high SNR when $\sigma^4 << J^2\sigma_h^2\mu$, applying $\mu\sigma_h^2 = 1/K$, then $\sigma^4 << J^2/K$. According to (6) this happens when the reference $SNR >> K$. In this case we have a gain with respect to Rayleigh propagation provided that the UIT is correctly

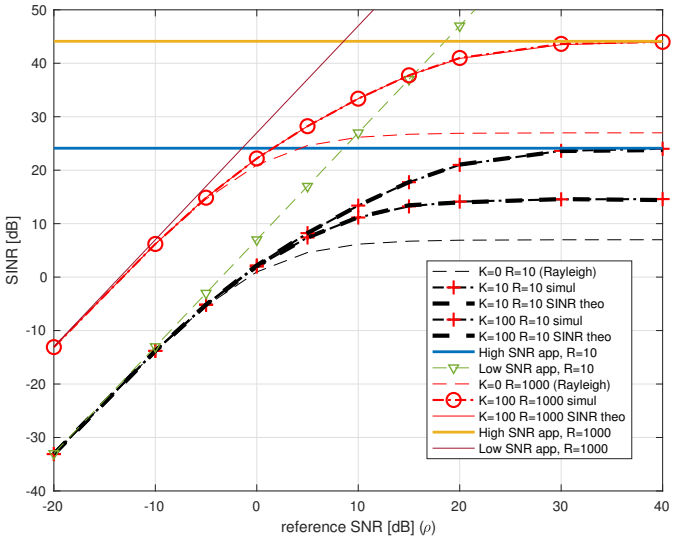

Fig. 3. SINR for perfectly Known UIT case.

C. Symbol Error Rate

We can assume that the interference plus noise defined in (17) is Gaussian due to the Central Limit Theorem. Therefore,

the error probability of the joint symbols $\varsigma[n]$ may be found using the Union Bound as was shown in [11]. By considering the minimum distance of the constellation between the symbols ς_m and $\varsigma_{m'}$ as

$$d_{min} = min\{|\varsigma_m - \varsigma_{m'}|, 1 \leq m \leq \mathfrak{K}, 1 \leq m' \leq \mathfrak{K}, m' \neq m\}, \quad (33)$$

and being d^m_{min} the minimum distance of the constellation point m to its nearest neighbor, then we can use an approximated bound for symbol error rate (SER) [24] as follows

$$Pe \approx \frac{1}{\mathfrak{K}} \sum_{m=0}^{\mathfrak{K}-1} Q\left(\frac{d^m_{min}}{\sqrt{2I}}\right). \quad (34)$$

The variable $I \in \{I^{worst}_{total}, I^{ideal}_{total}\}$ in (34) represents the interference plus noise for each of the two cases that were studied in previous sections. Their performance will be analyzed in Section VI.

The same approximation also applies to the individual SER of each of the users, provided that the distances between the constellation points that encode the same user's symbol are not evaluated.

IV. Constellation Design

Our previous designs [11] achieved a good performance with a reasonable number of antennas required in Rayleigh fading. When we have Rician channel, our designs remain valid in single user systems [16], but they are not applicable when we have a multi-user system due to the new IUI terms introduced by the LOS component, as we will show next.

As it was done in [7], for energy detection, when the channel is Rice we need to redesign the constellation based on DPSK. Here we propose a new design and we provide some general guidelines for further designs.

A. Previous design

In [11] we chose an approach where all users have the same error performance. This design was called *Equal Error Protection* (EEP). Hence, the constellation $\mathfrak{M}_j$ for user j is defined as

$$\mathfrak{M}^{EEP}_j = \left\{ \frac{2\pi[(m+1)J - 1 + j]}{JM}, m = 0, 1, ..., M-1 \right\} j = 1, ..., J, \quad (35)$$

In this design, the users symbols are intercalated in the unit circle, keeping equal distance among them. Fig. 4 shows for $M = 2$ and $J = 2$ the received constellation with UIT and neglecting the interference terms that vanish with increasing R. The red stars denote the position of the joint symbol plus interference computed from (14) and (16) as:

$$\varsigma[n] + UIT[n] = \varsigma[n] + \mu^2\varsigma[n] = (1 \pm \mu^2)\varsigma[n]. \quad (36)$$

The UIT defined in (16) depends on the information symbols transmitted by each user:

- The UIT coincides with the joint symbol ς when both users transmit the same or opposite symbol in two consecutive time instants resulting in a positive sign $(+\mu^2)$ in (36):

$$UIT[n] = \varsigma[n] \quad when \quad \begin{cases} s_j[n] = s_j[n-1] & or \\ s_j[n] = -s_j[n-1] & \forall j \end{cases} \quad (37)$$

- The UIT is opposite to the joint symbol $(-\varsigma)$ when one user transmits the same symbol and the other user transmits opposite symbol in two consecutive time instants resulting in a negative sign in (36), $(-\mu^2)$:

$$UIT[n] = -\varsigma[n] \quad when \quad \begin{cases} s_j[n] = s_j[n-1] & and \\ s_k[n] = -s_k[n-1] & j \neq k \end{cases} \quad (38)$$

The issue in the design shown in Fig. 4 is that we have double symmetry with respect to the coordinate axes. Hence, in the case that the UIT is opposite to the joint symbol $(-\varsigma)$ the amplitud of the received joint symbol is reduced an amount of $1-\mu^2$, more reduced as the LOS increases. Therefore ς plus UIT converges to zero as $(\mu \to 1)$, making impossible to decode the users information.

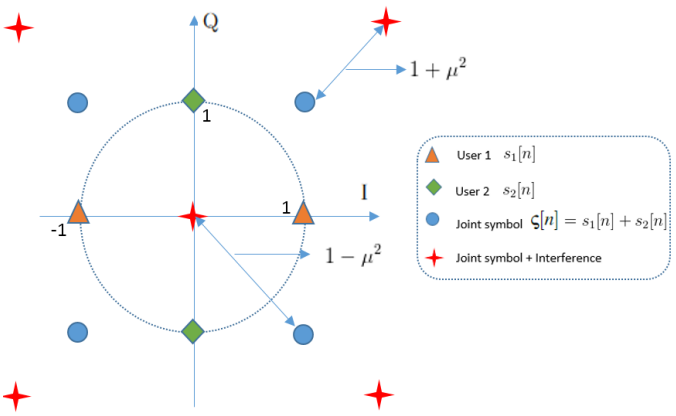

Fig. 4. Constellation for J =2 users and $M = 2$ valid for Rayleigh case but not for Rice case.

B. New design

In order to solve the problem of interference due to the LOS component we present a new design. In Fig. 5 an example is shown for $J = 2$ users and $M = 2$. The full constellation for one user (*e.g.* green diamond in Fig. 5 (a)) is intertwined with another user (orange triangles in Fig. 5 (a)), instead of inserting each symbol one by one as in Fig. 4. More users $(J > 2)$ can be interspersed throughout in the unit circle. The blue circles represent the ideal joint constellation as in the Rayleigh case $(K = 0)$, but when we consider the effect of μ, the red stars appear in Fig. 5 (b). This is due to the UIT in (8) that is not cancelled by increasing R, but merely moves ς towards zero. Unlike in the constellation in Fig. 4, we have an unambiguous relation between users symbols and the joint symbols despite the UIT. In addition, extra symbols appear that help us for a more reliable decision since they give us information about the channel effects, that we will use in the detection algorithms.

This is due to the fact that we remove the double symmetry which showed Fig. 4.

We can note that in the first received symbol ($l = 1$) the UIT term is always known. In the particular case of two users ($J = 2$), $x_j[0] = 1$ and considering (1) we have

$$UIT(1) = x_1[1]x_2^*[0] + x_2[1]x_1^*[0] = \\ = s_1[1]x_1^*[0]x_2^*[0] + s_2[1]x_2^*[0]x_1^*[0] = s_1[1] + s_2[1] = \varsigma[1] \quad (39)$$

Then, the received symbol has no IUI but is just amplified, case $(1+\mu^2)\varsigma$ in (36). We will make use of this property in the proposed detection algorithm in section V.C

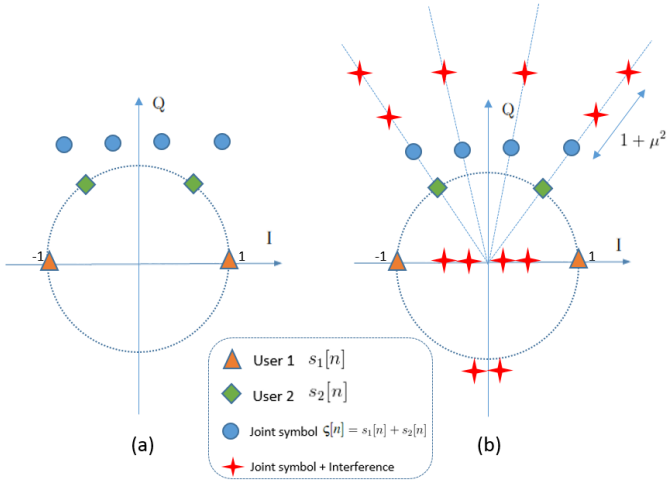

Fig. 5. New Constellation Design for J =2 users and $M = 2$. (a) For Rayleigh case. (b) For Rice case.

C. Considerations for MU NC m-MIMO

Here, for the sake of space, we will only show the performance for the new design explained in Section III.B. However, we can offer several considerations which have to be taken into account when designing a different constellation to work with a Rician fading.

1) In general, all individual constellations $\mathfrak{M}_j$ must be designed so that their symbols do not overlap after adding the transmitted signals from all users at the BS, in order to separate the users' signals.
2) The joint constellation can not display a double symmetry with respect to the coordinate axes. One possible option is intercalating the symbols of a given user between two symbols of the previous user to avoid the symmetry.
3) The best solution is obtained with the same distance among the symbols of the same users (maximizing the minimum distance).
4) Using the half plane for allocating each user is more recommendable because the joint symbols are better distributed and remain unambiguously detectable even with the interference.

In addition, we must bear in mind that the interference created by the LOS component is in general harmful, since it can cause that several different transmit symbols collapse to the same one at reception, making then impossible to detect.

TABLE I
SPECTRAL EFFICIENCY DUE TO THE INSERTION OF A REFERENCE SYMBOL

	$L=2$	$L=5$	$L=10$
Useful Rate	2/3	5/6	10/11

Therefore, by constellation design, the LOS component can be used to cause several different joint symbols corresponding to the same transmitted one, which helps us to make a more reliable decision, because it provides information about the interference itself.

V. DETECTION ALGORITHMS

In this section, we review classical algorithms which are well known in the literature and have been proposed to decode frames of L symbols ($l = 1...L$) for non-coherent multi-user schemes. We assume a frame is made of one reference symbol followed by L information symbols, then we have $L+1$ symbols per frame. In Table I we collect some examples for the spectral efficiency corresponding to different values of L. The classical algorithms have some drawbacks. Their complexity grows exponentially with L and they can not compensate the interference caused by Rician fading. Therefore, we propose a new algorithm to compensate this interference and even improve the performance with respect to the Rayleigh case.

A. Detection by L-symbol sequences

This technique consists in decoding sequences formed by multiple symbols instead of symbol-by-symbol, to reduce the effect of the UIT. However, independently of the chosen constellation, due to the fact that different combinations of user symbols may collapse to the same UIT after non-coherent combination at the receiver, we may get the same sequence in reception for different transmitted symbols. Increasing L does not help, because it creates even higher probability of having some repeated sequences. Therefore, this detection technique does not offer a good performance in Rician channels.

B. Detection by double Minimum Distance (MD)

Another method is using a MD detector twice: one detector for the joint symbol, $\hat{\varsigma}_j$ and another MD detector for the UIT. Then we choose the minimum distance solution jointly as follows. For each received joint symbol, we choose a feasible value of UIT originating from the constellation in Fig. 5. Then, each UIT is subtracted to the received symbol ($z[n]$) in order to make a minimum distance detection comparing with the joint constellation $\mathfrak{M}$, obtaining a distance d_k, where the subindex k indexes the set of UIT values. We repeat this procedure for all possible UIT values. Finally, we select the estimated joint symbol corresponding to the minimum d_k. For the case $K = 0$, we do not have the UIT term, therefore the decoding procedure boils down to the one in [11]. The main problem is the error propagation (EP), because we are doing symbol-by-symbol detection, taking a decision based on the previous symbol.

C. Proposed JSD Algorithm

It is noticed from (8) that non-coherent differential detection causes extra interfering terms with respect to the Rayleigh case. It was not possible to cancel such terms using classical algorithms. Therefore, we avail of the new joint constellation of Fig. 5 to improve the decision. Recall that Fig. 5 shows an extended constellation that considers all possible received points due to all possible experienced UIT values. Hence, by using this constellation, the originally transmitted symbols are detected without knowing the actual UIT that took place. This is done for the first two symbols of each sequence of L, relying on the decision of $l = 1$ to improve the decision of $l = 2$. With these decisions, we provide a reduction of the possible received sequences, avoiding their repetition. By analyzing how this UIT progresses as the users transmit information symbols, we have decided to restrict the detection of UIT for the first two symbols. Extending it to $l = 3$ would increase seriously the complexity and errors may propagate from the decision $l = 2$ to $l = 3$. Since differential encoding is employed we may have EP. In order to avoid the effect of the EP, a decision can be based on a number of consecutive symbols just like in [6] with multi-symbol differential detector, once we have avoided the repetition of sequences with the decision of the first two symbols. The number of symbols which are used in the detection is L. The new algorithm consists in the next steps:

1) The first symbol ($l = 1$) can be obtained directly by dividing the received symbol by $1+\mu^2$, followed by a minimum distance detection using the constellation in Fig. 5 (a) since there is not IUI yet.
2) For $l = 2$, we take a decision according to:
   - **2.**1 Select the sequence with minimum distance among all possible resulting sequences of any $L = 2$ symbols of the extended joint constellation (Fig. 5 (b)).
   - **2.**2 We compare the symbol corresponding for $l = 1$ in the selected sequence in 2.1 with the step before.
     a) In the case the symbol for $l = 1$ coincides with the decoded one in step 1: the selected sequence for $l = 2$ is correct.
     b) In the case the symbol for $l = 1$ does not coincide with step 1: select those sequences for $L = 2$ symbols matching with the decision for symbol $l = 1$ in step 1. Repeat a minimum distance based decision among all the sequences of the subset.
3) For $l > 2$, select the sequences whose $l = 1$ and $l = 2$ fit with those selected in step 1 and 2. Make a minimum distance decision with the subset of resulting sequences.

In Algorithm 1 a pseudocode is shown for the proposed non-coherent detection algorithm.

Algorithm 1 Non-coherent detection of sequences with $L > 2$ symbols for JSD Algorithm.

Input Data: received L symbols: $z[1],...,z[L]$
Result: $b_1^j,...,b_p^j$ for j=1, ..., J
Initialization
Step 1: decoding symbol 1 **is**
    $z[1]/(1+\mu^2)$
    MD using constellation Fig. 5 (a)
    return $\hat{s}_j[1]$
end
Step 2: decoding symbol 2 **is**
    MD using constellation Fig. 5 (b) **return** $s_j^*[1], s_j^*[2]$
if $s_j^*[1] = s_j[1]$ **then**
  sequence correct
  $\hat{s}_j[1] = s_j^*[1]$ and $\hat{s}_j[2] = s_j^*[2]$
else
  subset: sequences of $L = 2$ symbols with $s_j[1]$ **from** step1
  multiple-sequence MD with subset using constellation Fig. 5 (b) $\hat{s}_j[1] =$ step 1 and $\hat{s}_j[2] = s_j^*[2]$
end if
    return$\hat{s}_j[1]$ and $\hat{s}_j[2]$
end
Step 3: decoding symbol $l > 2$ **is**
    subset: sequences of L with $\{s_j[1],s_j[2]\}$ **from** step2;
    MD using constellation Fig. 5 (b)
    return $\{\hat{s}_j[1]$, ..., $\hat{s}_j[L]\}$
end
Binary Conversion : $\hat{s}_j[n] \rightarrow \hat{b}_1^j,...,\hat{b}_p^j$

D. Complexity analysis

We compare the computational complexity of our proposed algorithm with those of conventional algorithms. We study the complexity dependency with the number of symbols per frame (L), the order of the constellation (M), and the number of users (J). For these parameters of the system, we calculate the number of comparisons that must be performed between each received frame of symbols with all possible transmitted sequences.

For the first classical algorithm, detection by L-symbol sequences, the number of comparisons required is M^{JL}. For the classical second algorithm, the complexity is $M^{J(l+1)}$ for the l^{th}-symbol and the complexity required to detect the total L received symbols is $M^J + \sum_{l=2}^{L} M^{J(l+1)}$.

The complexity of our proposed JSD algorithm is calculated in 2 phases: first for $l = 2$ it is the same as for the detection by L-symbol sequences since we have to compare with all the possible symbols of the new constellation, this is M^{2J}. In the second phase, once the symbols 1 and 2 are detected, we make $M^{J(L-2)}$ comparisons with the remaining subset. Then the complexity is $M^{2J} + M^{J(L-2)}$. Compared to the first detection algorithm we obtain a reduction of 92% in calculations. Compared to the detection by double MD algorithm we obtain the reduction of 98%. For example: when we receive a sequence of $L = 5$ symbols for $M = 2$ and $J = 2$, our proposed JSD algorithm makes 80 comparisons against 1024 and 5444 comparisons in the $L-$symbol algorithm and MD respectively.

VI. Performance Results

In this section we examine the performance of our design in a two-user ($J = 2$) uplink with frequency-flat Rician fading,

where a random channel is generated at each iteration following the model explained in Section II and it is kept constar for L consecutive transmitted symbols (block fading), for minimum of 100,000 iterations. The channels correspondin to the transmission form each of the two users are uncorrelate and they have the same K factor (with values 0, 1, 5, 10, 50 an 100) following equations (2) and (3). The constellation orde of the users signals M varies from 2 to 8 and the number c antennas at the BS is changed between $R = 10$ and $R = 1000$

Firstly, we analyze the SER obtained by the previou classical algorithms. In the case of detection by L-symbc sequences, Fig. 6 shows that the detection is possible onl for sequences of $L = 2$ symbols and increasing the K factc helps to improve the performance. However, when L increase there is a number of antennas R from which the performanc worsens when K increases, that is the detection by sequence does not help when we have a Rice fading. In particular, w can see in Fig. 6 that for $L \geq 10$ and $R > 100$ the performanc for $K = 10$ is worse than for Rayleigh propagation ($K = 0$) i [11]. Alternatively, we can use MD as shown in Fig. 6. In thi, case, the SER for the case of $J = 2$ users and a Rician factor of $K = 10$ is shown. We can see a strong degradation in the performance as L increases, remaining the same from $L \geq 8$, due to the fact that the EP increases for longer frames. Again, this technique does not offer a good performance for Rician

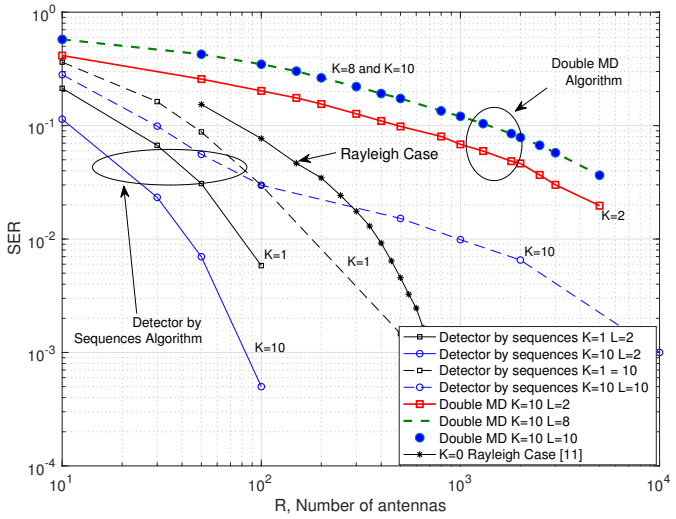

Fig. 6. Comparison of SER in classical algorithms for $J = 2$ users, $\rho = 0$ and $M = 2$ as L and K values.

Now, we examine the performance of the proposed JSD algorithm with the new constellation. First we verify the accuracy of the detection of the first two symbols, since the remaining ones depend on them. In Fig. 7 the SER when only decoding the first symbol ($l = 1$) is shown, corresponding to the first step in JSD algorithm. $R = 50$ antennas is used for three constellation sizes ($M = 2, 4$ and 8-DPSK) and different fading factors. We can see that even for very low SNR, we can correctly detect the first symbol. Moreover, the performance improves when increasing K factor up to $K = 5$ where it saturates. Hence the IUI does not affect the detection in this first step due to the fact that the UIT coincides with the first transmitted symbol.

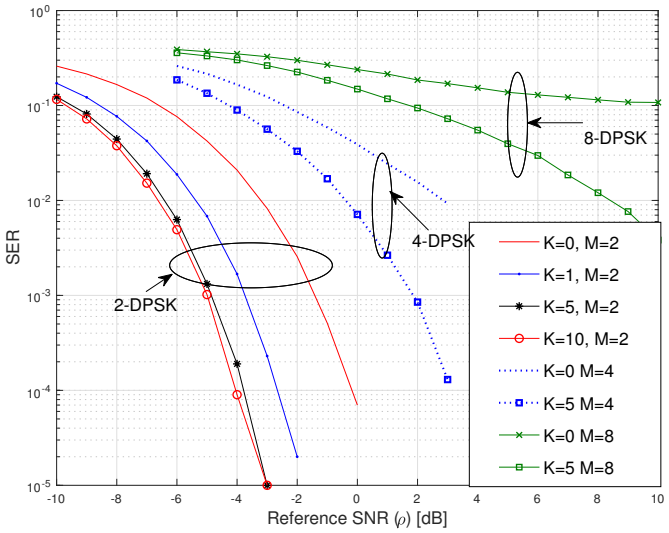

Fig. 7. SER for first symbol, J=2 users, R=50 antennas and M=2, 4 and 8.

Next, we validate in Fig. 8 the second step in the JSD algorithm, that is detecting the second symbol ($l = 2$), by means of the SER. We can see that using the knowledge of the first symbol helps us to detect the second one. Again, the performance improves when increasing K factor up to $K = 10$ where it saturates in this case. This contrasts with the performance of [7] where a value of $K > 100$ is needed to obtain an advantage with respect to Rayleigh propagation.

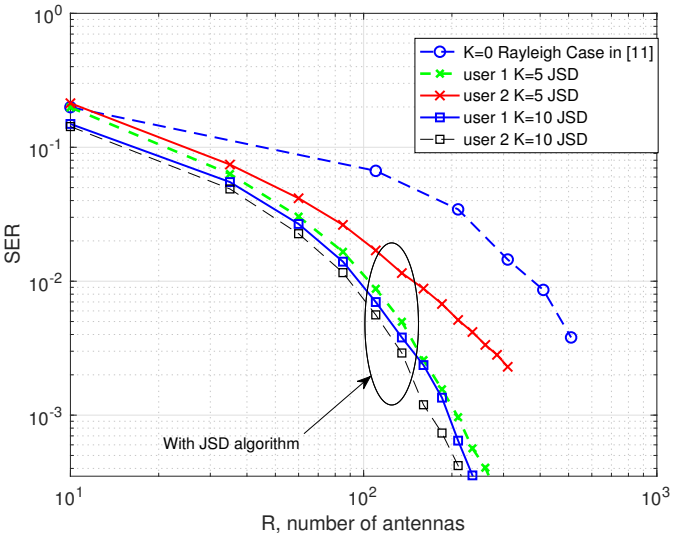

Fig. 8. SER for second symbol detected, $J = 2$ users, $\rho = 0$ dB, $M = 2$.

Once we have validated the detection of the first two symbols, we present in Fig. 9 the SER when detecting the complete sequence of $L = 5$ symbols for $K = 1$ and $SNR = 0$ dB. We can see that JSD offers a better performance than the two conventional algorithms as R increases. In this figure we also show the theoretical SER corresponding to considering UIT as interference (worst case), that is, using the SINR of (25) in (33) and the theoretical SER obtained when UIT is

perfectly known (ideal case), that is, using the SINR of (29) We can see that with JSD we practically approach the boun defined by (29).

Fig. 10 shows the SER and bounds for $K = 10$ an $SNR = 0$ dB. Again, we can see that our scheme outperform the conventional ones. The performance improves when L increases in our JSD algorithm, unlike in classical algorithms In particular, for $L = 2$ we have a performance that is slightly worse than the theoretical bound of (29), for $L = 5$ it i practically approaching the bound (29), while with $L = 1$ we even outperform this bound, meaning that we are abl to not only cancel but make use of the UIT to improve th performance.

The performance in Rayleigh and Rice channels is furthe examined in Fig. 11 where we plot the SER of (33) with SINR (29), that is, when UIT is perfectly known. In this figure $\rho = -3dB$ and $3dB$, $J = 2$ users and a higher order constellation $M = 4$ is used. We can see that for very low SNR the K facto does not influence the performance, as we anticipated in Fig. 3. When we increase the SNR, the Rician propagation helps to improve the performance.

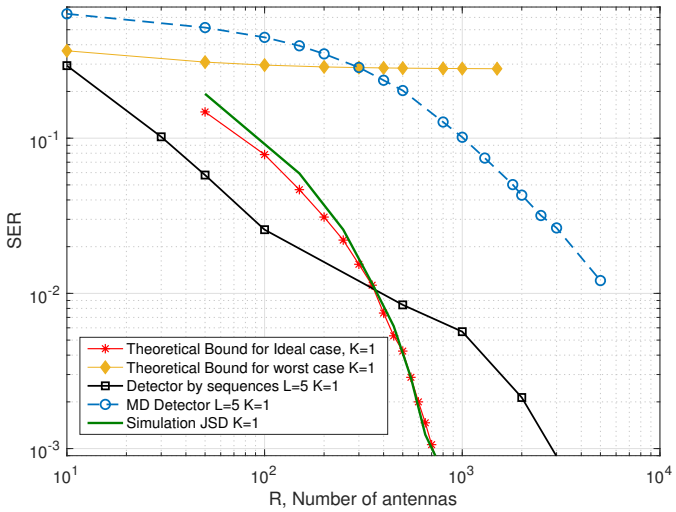

Fig. 9. SER for $K = 1$ with $J = 2$ users, $\rho = 0$ dB, $M = 2$ and $L = 5$.

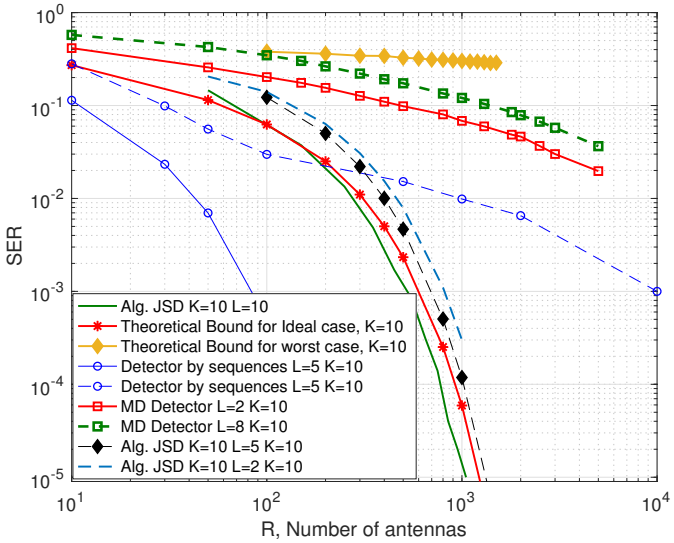

Fig. 10. SER for $K = 10$ with $J = 2$ users, $\rho = 0$ dB, $M = 2$ and $L = 5$.

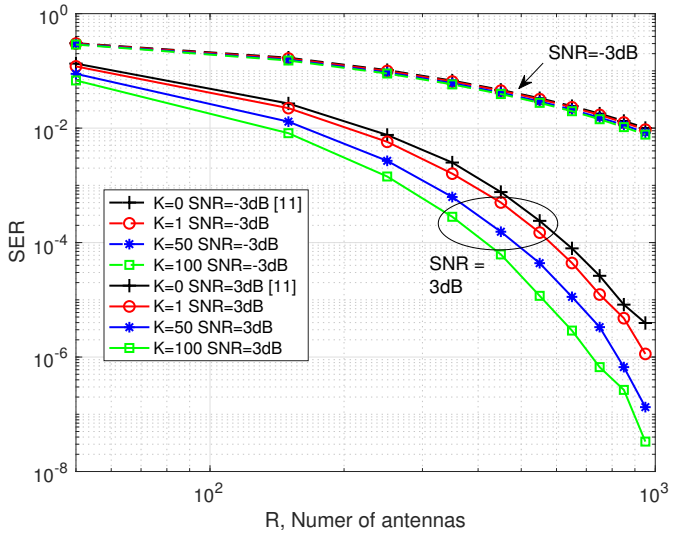

Fig. 11. SER for perfectly known UIT (ideal case) with $J = 2$ users, $M = 4$.

VII. Conclusions

In this paper, we have presented a new constellation for a multi-user non-coherent massive SIMO system with M-DPSK that can be used in Rician channels. This constellation allows an unambiguous detection of the transmitting symbols despite the interference caused by the LOS component. Furthermore, we have proposed a detection algorithm based on the multi-symbol joint decision enhanced with the knowledge of the new constellation and the effect of interference. The SINR and SER have been theoretically analyzed showing a good match with the simulations. We have analyzed the performance of the system showing an improvement with respect to classical non-coherent detection techniques. With the proposed constellation and detection algorithm we are able to leverage the LOS component of the Rician propagation, obtaining a better performance than with Rayleigh channels. This better performance translates to a decrease of the required number of antennas. Furthermore, we have seen that the designs based on M-DPSK outperform those based on energy detection [7] and [22] also in Rician propagation.

Appendix
Derivation of the Interference Plus Noise Power

In this appendix, we outline the derivation of the power of the different terms of $i[n]$, $I = E\{|i[n]|^2\}$ which were presented in Section III. For I_0, since $E\{x_j^*[n-1]x_k[n]\} = 0$ for $j \neq k$, we have

$$I_0 = E\left\{\left|\sum_{j=1}^{J} s_j[n]\left(1 - \frac{1}{R}\sum_{r=1}^{R}|h_{rj}|^2\right)\right|^2\right\} = \frac{J\sigma_h^2\mu}{R} \qquad (40)$$

because $E\{\sum_{r=1}^{R}|h_{rj}|^2\}=R$ and $E\{(\sum_{r=1}^{R}|h_{rj}|^2)^2=R(R+1)$ for $h_{rj}\sim CN(0,\sigma_h^2)$ [23]. For I_1 we have

$$\begin{aligned}E\left\{\left|\frac{1}{R}\sum_{j\neq k}^{J}\sum_{r=1}^{R}h_{rj}^{*}h_{r,k}x_j^{*}[n-1]x_k[n]\right|^2\right\}=\\=\frac{1}{R^2}E\left\{\sum_{j\neq k}^{J}\sum_{r=1}^{R}|h_{rj}|^2|h_{rk}|^2\right\}=\frac{J\sigma_h^4}{R},\end{aligned}\tag{41}$$

because

$$E\left\{h_{rj}h_{rk}^{*}h_{lj}h_{lk}^{*}\right\}=\begin{matrix}0,r\neq l\\\sigma_h^2,r=l\end{matrix}\tag{42}$$

For I_2, since $E\{v_r^{*}[n-1]v_r[n]\}=0$, $v_r[n]\sim CN(0,\sigma^2)$ and $h_{rj}\sim CN(0,\sigma_h^2)$, we have

$$\begin{aligned}I_2=E\left\{\left|\frac{1}{R}\sum_{r=1}^{R}\nu_r^{*}[n-1]\sum_{j=1}^{J}h_{r,j}x_j[n]+\frac{1}{R}\sum_{r=1}^{R}\nu_r[n]\sum_{j=1}^{J}h_{r,j}^{*}x_j^{*}[n-1]\right|^2\right\}\\=\frac{2}{R^2}E\left\{\left|\sum_{r=1}^{R}\nu_r^{*}[n-1]\sum_{j=1}^{J}h_{r,j}x_j[n]\right|^2\right\},\end{aligned}\tag{43}$$

and because $E\{|h_{rj}|^2\}=\sigma_h^2$ and $E\{|x_j[n]|^2\}=1$, we have

$$I_2=\frac{2J\sigma_h^2\sigma^2}{R}.\tag{44}$$

For I_3, since $v_r[n-1]$ and $v_r[n]\sim CN(0,\sigma^2)$ are independent, we have

$$\begin{aligned}I_3=E\left\{\left|\frac{1}{R}\sum_{r=1}^{R}\nu_r^{*}[n-1]\nu_r[n]\right|^2\right\}\\=\frac{1}{R^2}\sum_{r=1}^{R}E|v_r^{*}[n-1]|^2E|v_r[n]|^2=\frac{1}{R}\sigma^4.\end{aligned}\tag{45}$$

On the other hand, we derivate for the new interfering terms due to the LOS component. We must keep in mind the independence between two consecutive time instant n and $n+1$ for h_{rj} and x_j, then

$$\begin{aligned}I_4=2E\left\{\left|\frac{\mu}{R}\sum_{r=1}^{R}\sum_{j=1}^{J}\sum_{\substack{k=1\\k\neq j}}^{J}h_{rj}x_j[n]x_k^{*}[n-1]\right|^2\right\}=\\=\frac{2\mu^2}{R^2}E\left\{\sum_{r=1}^{R}\sum_{j=1}^{J}\sum_{\substack{k=1\\k\neq j}}^{J}|h_{rj}|^2|x_j[n]|^2|x_k[n-1]|^2\right\}=\\=\frac{2\mu^2J(J-1)\sigma_h^2}{R}.\end{aligned}\tag{46}$$

Similarly for I_5, the terms $v_r[n]$ and $x_j[n]$ are independent, then

$$\begin{aligned}I_5=2E\left\{\left|\frac{\mu}{R}\sum_{r=1}^{R}\sum_{j=1}^{J}x_j[n]v_r^{*}[n-1]\right|^2\right\}=\\=\frac{2\mu^2}{R^2}E\left\{\sum_{r=1}^{R}\sum_{j=1}^{J}|x_j[n]|^2|v_r^{*}[n-1]|^2\right\}=\\=\frac{2\mu^2\sigma^2J}{R}.\end{aligned}\tag{47}$$

Regarding to the term independent of the number of antennas we have

$$\begin{aligned}I_{UIT}=E\left\{\left|\sum_{j=1}^{J}\sum_{\substack{k=1\\k\neq j}}^{J}x_j[n]x_k^{*}[n-1]\right|^2\right\}=\\=\mu^4E\left\{\sum_{j=1}^{J}\sum_{\substack{k=1\\k\neq j}}^{J}|x_j[n]|^2|x_k^{*}[n-1]|^2\right\}=J(J-1)\mu^4\end{aligned}\tag{48}$$

Also, we demonstrate that the interference plus noise components are independent and uncorrelated in order to be able to add them. To this end, they have to fulfill

$$\begin{aligned}Cov(i_x,i_y)=E\{i_x[n]i_y[n]\}-E\{i_x[n}E\{i_y[n\}=0\\E\{i_x[n]i_y[n]\}=E\{i_x[n}E\{i_y[n\}\end{aligned}\tag{49}$$

for any $(x,y)=\{x=1,...,5$ and $y=1,...,5\}$ and where $Cov(a,b)$ is the covariance between the random variables a and b.

First, let us obtain the expectation for each term.

$$\begin{aligned}E\{i_0[n]\}=E\{\sum_{j=1}^{J}[s_j[n](1-\frac{1}{R}\sum_{r=1}^{R}|h_{rj}|^2)]\\-\frac{1}{R}\sum_{j=1}^{J}\sum_{\substack{k=1\\k\neq j}}^{J}\sum_{r=1}^{R}h_{rj}^{*}h_{rk}x_j^{*}[n-1]x_k[n]\}\\=\sum_{j=1}^{J}E\{s_j[n]\}-\frac{1}{R}E\{\sum_{r=1}^{R}|h_{rj}|^2\}\\-\frac{1}{R}\sum_{j=1}^{J}\sum_{\substack{k=1\\k\neq j}}^{J}\sum_{r=1}^{R}E\{h_{rj}^{*}h_{rk}x_j^{*}[n-1]x_k[n]\}\end{aligned}\tag{50}$$

where we assume that all constellation points s_j are independent and based on M-DPSK, then $E\{s_j[n]\}=1$.

In the last two lines in (50) we make use of the fact that the component h_{rj} and the noise v_i are independent and have zero mean so (50) results to be $E\{i_0[n]\}=0$.

Similarly, we derive the expectation for the second term as follows

$$
\begin{aligned}
E\{i_2[n]\} =& E\{-\frac{1}{R}\sum_{r=1}^{R}\nu_i^*[n-1]\sum_{j=1}^{J}h_{r,j}x_j[n] \\
&-\frac{1}{R}\sum_{r=1}^{R}\nu_i[n]\sum_{j=1}^{J}h_{rj}^*x_j^*[n-1]\} \\
=&-\frac{1}{R}\sum_{r=1}^{R}\sum_{j=1}^{J}E\{\nu_i^*[n-1]h_{rj}x_j[n]\} \\
&-\frac{1}{R}\sum_{r=1}^{R}\sum_{j=1}^{J}E\{\nu_i[n]h_{rj}^*x_j^*[n-1]\} \\
=&-\frac{1}{R}\sum_{r=1}^{R}\sum_{j=1}^{J}E\{\nu_i^*[n-1]\}E\{h_{rj}x_j[n]\} \\
&-\frac{1}{R}\sum_{r=1}^{R}\sum_{j=1}^{J}E\{\nu_i[n]\}E\{h_{rj}^*x_j^*[n-1]\}
\end{aligned}
\tag{51}
$$

By applying the independence between the $h_{r,j}$ and the noise, we have

$$
\begin{aligned}
E\{i_2[n]\} =& -\frac{1}{R}\sum_{r=1}^{R}\sum_{j=1}^{J}E\{\nu_i^*[n-1]\}E\{h_{rj}x_j[n]\} \\
&-\frac{1}{R}\sum_{r=1}^{R}\sum_{j=1}^{J}E\{\nu_i[n]\}E\{h_{rj}^*x_j^*[n-1]\}
\end{aligned}
\tag{52}
$$

then as $E\{\nu_i^*[n]\}=0$, so finally $E\{i_2[n]\}=0$.

For the third term, the expectation is

$$
\begin{aligned}
E\{i_3[n]\} =& E\{-\frac{1}{R}\sum_{r=1}^{R}\nu_i^*[n-1]\sum_{j=1}^{J}h_{rj}x_j[n] \\
&-\frac{1}{R}\sum_{r=1}^{R}\nu_i[n]\sum_{j=1}^{J}h_{rj}^*x_j^*[n-1]\} \\
=&-\frac{1}{R}\sum_{r=1}^{R}\sum_{j=1}^{J}E\{\nu_i^*[n-1]\}E\{h_{rj}x_j[n]\} \\
&-\frac{1}{R}\sum_{r=1}^{R}\sum_{j=1}^{J}E\{\nu_i[n]\}E\{h_{rj}^*x_j^*[n-1]\}
\end{aligned}
\tag{53}
$$

that results in $E\{i_3[n]\}=0$.

The rest of ones, under the same conditions as in previous terms, the independence of h_{rj}, noise v_j and symbols x_j, the expectation is zero also. The multiplier effect of μ does not affect in this derivation.

Once the expectation is derived, the cross expectations of each of the terms have to fulfill

$$
E\{i_x[n]i_y[n]\}=0 \tag{54}
$$

In the next page, some example cross expectations is used to illustrate it.

Due to the independence between the channel and the noise, the cross terms (55), (56) and (57) are zero, therefore the expressions in (54) is fulfilled for any pair. Hence the interference terms are uncorrelated and they can be linearly added.

REFERENCES

[1] E.G. Larsson, O. Edfors, F. Tufvesson, and T.L. Marzetta, "Massive MIMO for Next Generation Wireless Systems," *IEEE Comm. Mag.*, vol. 52, no. 2, pp. 186-195, Feb. 2014.

[2] Y. Li, P. Fan, A. Leukhin, and L. Liu, "On the spectral and energy efficiency of full-duplex small-cell wireless systems with massive MIMO," *IEEE Trans. Vehicular Technology*, vol. 66, no. 3, pp. 2339-2353, Mar. 2017.

[3] 3GPP TS 36.211, "LTE; Evolved Universal Terrestrial Radio Access (E-UTRA); Physical channels and modulation," v.10.0.0 Rel. 10, Jan. 2011.

[4] X. Dai, Z. Zhang, S. Chen, S.Sun and B. Bai, "Pattern Division Multiple Access (PDMA): A New Multiple Access Technology for 5G," *IEEE Wire. Commun.*, vol. 25, pp. 54-60, Apr. 2018.

[5] J. Zhang, B. Zhang, S. Chen, X. Mu, M. El-Hajjar, and L. Hanzo, "Pilot contamination elimination for large-scale multiple-antenna aided OFDM systems," *IEEE J. Sel. Topics Signal Process*, vol. 8, pp. 759-772, Oct. 2014.

[6] L. Wang, L. Li, C. Xu, D. Liang, S. Xin and L. Hanzo, "Multiple-Symbol Joint Signal Processing for Differentially Encoded Single- and Multi-Carrier Communications: Principles, Designs and Applications," *IEEE Communications Survey & Tutorials*, vol. 16, no. 2, pp. 689-712, Feb. 2014.

[7] Alexandros Manolakos, Mainak Chowdhury, Andrea Goldsmith, "Energy-based Modulation for Noncoherent Massive SIMO Systems," *IEEE Trans. on Wireless Communications*, vol. 15, Nov. 2016.

[8] B. Knott, M. Chowdhury, A. Manolakos and A.J. Goldsmith, "Benefits of Coding in a Noncoherent Massive SIMO System," *IEEE ICC*, pp. 2350-2355, Jun. 2015.

[9] E. Leung, Z. Dong and J.K. Zhang, "Uniquely Factorable Hexagonal Constellation Designs for Noncoherent SIMO Systems," in *IEEE Trans. Vehicular Technology.*, vol. 66, pp. 5495-5501, Nov. 2016.

[10] A. G. Armada and L. Hanzo, "A Non-Coherent Multi-User Large Scale SIMO System Relying on M-ary DPSK," *IEEE ICC*, Jun.15 pp 2517-2522.

[11] V. M. Baeza, A. G. Armada, W. Zhang, M. El-Hajjar and L. Hanzo, "A Non-Coherent Multi-User Large Scale SIMO System Relying on M-ary DPSK and BICM-ID," *IEEE Trans. on Vehicular Technology*, vol. 67, pp.1809-1814, Sep. 2017.

[12] J. Camp and E. Knightly, "Modulation rate adaptation in urban and vehicular environments: Cross-layer implementation and experimental evaluation," *IEEE Trans. on ACM Networking*, vol. 18, no. 6, pp. 1949-1962, Dec. 2010.

[13] H. Zhang, Y. Liao and Lingyang Song, "D2D-U: Device-to-Device Communications in Unlicensed Bands for 5G System," in *IEEE Trans. on Wireless Communications*, vol. 16, pp 3507-3519, Mar. 2017.

[14] S. Hur et al., "Proposal on millimeter-wave channel modeling for 5G cellular system," *IEEE J. Sel. Topics Signal Process.,* vol. 10, no. 3, pp. 454-469, Apr. 2016.

[15] S. Sun, T. Rappaport, M. Shafi, P. Tang, J. Zhang and P.J. Smith , "Propagation Models and Performance Evaluation for 5G Millimeter-Wave Bands," *IEEE Trans. on Vehicular Technology*, vol. 1, pp.1-17, Jul. 2018.

[16] V.M. Baeza and A.G. Armada "Analysis of the Performance of a Non-Coherent Large Scale SIMO System Based on M-DPSK Under Rician Fading," *EUSIPCO*, vol. 1, pp-1-6, Kos Sep, 2017.

[17] M. Matthaiou, P. J. Smith, H.Q. Ngo and H. Tataria, "Does Massive MIMO Fail in Ricean Channels?," *IEEE Wireless Communication Letters* vol. 1, pp 1-4, Jul. 2018.

[18] S. Jin, D. Yue, H. Nguyen, "Equal-Gain Transmission in Massive MIMO Systems under Ricean Fading," *IEEE Trans. on Vehicular Technology* vol. 1, pp 1-10, Jul. 2018.

[19] Y. Wang and Z. Tian, "Multiple Symbol Differential Detection for Noncoherent Communications With Large-Scale Antenna Arrays," in *IEEE Wireless Communications Letters*, vol. 7, pp 190-193, Apr. 2018.

[20] V.M. Baeza, A.G. Armada, M. El-Hajjar and L. Hanzo, "Performance of a Non-Coherent Massive SIMO M-DPSK System," *Vehicular Technology Conference*, Sep. 2017.

[21] A. J. Goldsmith, "Wireless communications." Cambridge University Press, 2005.

[22] H.Q. Ngo, E.G. Larsson, and T.L. Marzetta, "Energy and spectral efficiency of very large multiuser MIMO systems," *IEEE Trans. Commun.*, vol. 61, no. 4, pp. 1436-1449, Apr. 2013.

[23] A.M. Tulino, S. Verdu, "Random matrix theory and Wireless Communications," *Foundations and Trends in Communications and Information Theory*, vol. 1, no. 1, pp. 1-182, 2004.

$$E\{i_0[n]i_3[n]\} = -\frac{1}{R}\sum_{j=1}^{J}\sum_{r=1}^{R}E\{s_j[n]\}E\{\nu_i^*[n-1]\}E\{\nu_i[n]\} + \frac{1}{R^2}\sum_{j=1}^{J}\sum_{r=1}^{R}\sum_{r=1}^{R}E\{\nu_i^*[n-1]\}E\{\nu_i[n]\}E\{|h_{rj}|^2 s_j[n]\} + \frac{1}{R^2}\sum_{j=1}^{J}\sum_{\substack{k=1\\k\neq j}}^{J}\sum_{r=1}^{R}\sum_{r=1}^{R}E\{h_{rj}^*\}E\{h_{rk}\}E\{x_j^*[n-1]x_k[n]\}E\{\nu_i^*[n-1}E\{\nu_i[n]\} \tag{55}$$

$$\begin{aligned}E\{i_0[n]i_2[n]\} =& E\{-\sum_{j=1}^{J}s_j[n]\frac{1}{R}\sum_{r=1}^{R}\nu_r^*[n-1]\sum_{j=1}^{J}h_{rj}x_j[n] - \sum_{j=1}^{J}s_j[n]\frac{1}{R}\sum_{r=1}^{R}\nu_r[n]\sum_{j=1}^{J}h_{rj}^*x_j^*[n-1] + \sum_{j=1}^{J}\frac{1}{R}\sum_{r=1}^{R}|h_{rj}|^2\frac{1}{R}\sum_{r=1}^{R}\nu_r^*[n-1]\sum_{j=1}^{J}h_{rj}x_j[n]\\ &+ \sum_{j=1}^{J}\frac{1}{R}\sum_{r=1}^{R}|h_{rj}|^2\frac{1}{R}\sum_{r=1}^{R}\nu_r[n]\sum_{j=1}^{J}h_{rj}^*x_j^*[n-1] + \frac{1}{R}\sum_{j=1}^{J}\sum_{\substack{k=1\\k\neq j}}^{J}\sum_{r=1}^{R}h_{rj}^*h_{rk}x_j^*[n-1]x_k[n]\frac{1}{R}\sum_{r=1}^{R}\nu_r^*[n-1]\sum_{j=1}^{J}h_{rj}x_j[n]\\ &+ \frac{1}{R}\sum_{j=1}^{J}\sum_{\substack{k=1\\k\neq j}}^{J}\sum_{r=1}^{R}h_{rj}^*h_{rk}x_j^*[n-1]x_k[n]\frac{1}{R}\sum_{r=1}^{R}\nu_r[n]\sum_{j=1}^{J}h_{rj}^*x_j^*[n-1]\}\end{aligned} \tag{56}$$

$$E\{i_2[n]i_3[n]\} = \left(\frac{1}{R}\sum_{r=1}^{R}E\{\nu_r^*[n-1]\}\right)^2\sum_{j=1}^{J}E\{h_{rj}\}E\{x_j[n]\}E\{\nu_r[n]\} + \left(\frac{1}{R}\sum_{r=1}^{R}E\{\nu_r[n]\}\right)^2\sum_{j=1}^{J}E\{\nu_r^*[n-1]\}E\{h_{rj}^*\}E\{x_j^*[n-1]\} \tag{57}$$

[24] J.G. Proakis, M. Salehi, *Digital Communications*, McGraw-Hill, NY, USA, 5th edition, 2007.